Uncertainty and data worth analysis for the hydraulic design of funnel-and-gate systems in heterogeneous aquifers

Olaf A. Cirpka,[1] Claudius M. Bürger,[2] Wolfgang Nowak,[3] and Michael Finkel[2]

Received 19 May 2004; revised 24 August 2004; accepted 13 September 2004; published 4 November 2004.

[1] Hydraulic failure of a funnel-and-gate system may occur when the contaminant plume bypasses the funnels rather than being captured by the gate. We analyze the uncertainty of capturing the plumes by funnel-and-gate systems in heterogeneous aquifers. Restricting the analysis to two-dimensional, steady state flow, we characterize plume capture by the values of the stream function at the boundaries of the plume and the funnels. On the basis of the covariance of the log conductivity distribution we compute the covariance matrix of the relevant stream function values by a matrix-based first-order second-moment method, making use of efficient matrix-multiplication techniques. From the covariance matrix of stream function values, we can approximate the probability that the plume is bypassing the funnels. We condition the log conductivity field to measurements of the log conductivity and the hydraulic head. Prior to performing additional measurements, we estimate their worth by the expected reduction in the variance of stream function differences. In an application to a hypothetical aquifer, we demonstrate that our method of uncertainty propagation and our sampling strategy enable us to discriminate between cases of success and failure of funnel-and-gate systems with a small number of additional samples. *INDEX TERMS:* 1829 Hydrology: Groundwater hydrology; 1869 Hydrology: Stochastic processes; 1832 Hydrology: Groundwater transport; *KEYWORDS:* conditioning, data worth, funnel-and-gate systems, heterogeneous aquifers, stream function, uncertainty propagation

Citation: Cirpka, O. A., C. M. Bürger, W. Nowak, and M. Finkel (2004), Uncertainty and data worth analysis for the hydraulic design of funnel-and-gate systems in heterogeneous aquifers, *Water Resour. Res.*, *40*, W11502, doi:10.1029/2004WR003352.

1. Introduction

[2] During the last 15 years, permeable reactive barriers have become an accepted technology for passive remediation of plumes in contaminated aquifers [*Day et al.*, 1999; *Gavaskar*, 1999; *Richards*, 2002]. The reactive barrier consists of a highly permeable material facilitating the decrease in the mass flux of a contaminant passing through the permeable reactive barrier. In the funnel-and-gate design, sheet piles or other hydraulic barriers are installed to guide the plume, which moves with natural groundwater flow, toward the in situ reactor [*Starr and Cherry*, 1994].

[3] Although numerous funnel-and-gate systems have been in operation over several years, open questions remain in their design and long-term performance. Here we focus on the probability that the plume indeed passes through the gate and does not bypass the funnels, due to heterogeneity of the aquifer. An example for this type of hydraulic failure was documented for the reactive barrier at Denver Federal Center in Denver, Colorado, where approximately 25% of the flux bypassed the funnel-and-gate system [*McMahon et al.*, 1999]. Hydraulic failure is of particular importance because the investment costs of funnel-and-gate systems are high. When the system is not capturing the plume, upgrading is more cost intensive than the upgrade of a comparable pump-and-treat system. For the evaluation of the funnel-and-gate design, calibrated numerical models for groundwater flow and solute transport are needed but may prove insufficient if the uncertainty of the model predictions is not quantified.

[4] Besides temporal fluctuations of the hydrological regime, a main cause of uncertainty in the hydraulic design of funnel-and-gate systems is the spatial variability of natural geological formations. With the effort typically used at a site, it is impossible to determine hydraulic aquifer parameters with a resolution that allows for deterministic modeling. The incomplete knowledge of aquifer properties leads to uncertain model predictions. Thus uncertainty has to be addressed in the design of in situ groundwater treatment systems.

[5] Previous studies on the reliability of permeable reactor barriers using funnel-and-gate systems in heterogeneous aquifers were based on Monte Carlo simulations, that is, the simulation of flow and transport using multiple, equally likely realizations of the conductivity field or reactions rates [*Eykholt et al.*, 1999; *Bilbrey and Shafer*, 2001; *Elder et al.*, 2002; *Bürger et al.*, 2003]. To obtain good estimates of uncertainty, however, at least a few hundred realizations are required. The latter is demonstrated, e.g., in the study of [*Bürger et al.*, 2003] who considered 500 unconditional realizations of hydraulic-conductivity fields and constructed reliability curves for different designs of funnel-and-gate systems. These calculations are computationally costly; each realization requires the simulation of groundwater flow

[1]Swiss Federal Institute for Environmental Science and Technology (EAWAG), Dübendorf, Switzerland.
[2]Center for Applied Geoscience, Universität Tübingen, Tübingen, Germany.
[3]Institut für Wasserbau, Universität Stuttgart, Stuttgart, Germany.

0043-1397/04/2004WR003352$09.00

and particle tracking for solute transport. When measurements of conductivities, heads, or concentrations are accounted for in the generation of the realizations, a conditioning step has to be added to each realization.

[6] In the present study, we approximate the uncertainty of the log hydraulic conductivity and its spatial correlation by the marginal covariance function of log conductivity. The marginal covariance summarizes the uncertainty caused by random fluctuations about the mean and the uncertainty in parameters describing large-scale trends. We propagate the uncertainty of log conductivity onto that of model outcomes, in which the latter are used to assess the hydraulic reliability, or failure, of the funnel-and-gate system. We apply first-order uncertainty propagation that does not require the simulation of multiple realizations. We account for measured data by conditioning, leading to a shift in the estimated parameter field and a reduction of the remaining uncertainty. The more measurements are accounted for, the smaller is the uncertainty. In any practical application, however, it will never become zero.

[7] In good engineering practice, uncertainty is addressed by the introduction of a margin of safety. In our case, the funnel-and-gate system has to be designed in such a way that more water passes through the gate than that within the width of the plume. A design may be defined reliable when the probability that clean water passes through the gate on both sides of the plume exceeds a defined threshold value. In this case, the volumetric fluxes of clean water passing the gate at both sides of the plume can be seen as the margins of safety. Obviously, more intensive site investigation reduces the uncertainty and thus allows for a design with a smaller safety factor. Since installing additional sampling wells is expensive, they should be placed at locations where the maximum reduction of uncertainty is expected.

[8] The determination of optimal sampling locations for hydrogeological applications has been studied earlier. In 1992, the Task Committee on Groundwater Quality Monitoring Network Design of the American Society of Civil Engineers (ASCE) published a review on groundwater sampling strategies [*Loaiciga et al.*, 1992], devoting a large section on statistical methods for the selection of optimal sampling locations. In our study, we essentially adopt the variance reduction analysis of *Rouhani* [1985]. It is widely recognized that the best additional sampling location does not only depend on the location of greatest parameter uncertainty, but also on the decision being made or the objective that it is sampled for [*Andricevic*, 1993; *Christakos and Killam*, 1993; *James and Gorelick*, 1994]. The known applications that are closest to our study address the detection of plumes or their boundaries [*Meyer and Brill*, 1988; *McGrath and Pinder*, 2003].

[9] In a full economical analysis, the worth of additional data points is quantified by the difference between the management costs at present information state and the expected management costs taking a sample at a particular location. The difference in costs is called the expected value of sample information [*Freeze et al.*, 1992; *James and Gorelick*, 1994]. The measurement location maximizing the expected value of sample information is chosen as the next sampling point, provided that the sampling is economically feasible. The computation of the expected costs requires a complete design optimization process for each possible outcome of the proposed measurement. Relying on nested optimization loops, such an analysis easily becomes unworkable due to the computational effort.

[10] In this study, rather than performing a full cost analysis, we adopt the standpoint of a decision maker who designed a funnel-and-gate system based on a deterministic, homogeneous model [*Starr and Cherry*, 1994; *Teutsch et al.*, 1997; *Sedivy et al.*, 1999], accounting for heterogeneity by a subjective safety factor. A rigorous stochastic analysis of the design based on the current information does not yield the targeted reliability. The decision maker is willing to spend an additional amount of money on site investigation and seeks guidance on where to place samples in order to gain the most decisive information about design functionality. In this sense, we evaluate the worth of additional data.

[11] Our analysis is restricted to steady state flow in essentially two-dimensional aquifers. Contaminant transport is assumed to be dominated by advection. This allows for using an advective control strategy [*Mulligan and Ahlfeld*, 1999] to check the functionality of a given funnel-and-gate design. While the method of *Mulligan and Ahlfeld* [1999] is based on particle tracking, we outline the boundaries of the contaminant plume by streamlines, that is contour lines of stream function values. Deterministic plume capture is considered achieved when the interval of the stream function values representing the bounding streamlines of the plume is a subset of the interval given by the two stream function values computed at the gate boundaries. We evaluate the uncertainty of stream function values by a matrix-based first-order second-moment method [*Dettinger and Wilson*, 1981] and derive a measure for the hydraulic reliability of the funnel-and-gate system. Conditioning to conductivity or head data is achieved by the quasi-linear method of geostatistical inversing [*Kitanidis*, 1995; *Nowak and Cirpka*, 2004]. The considered hydraulic head data are for the situation prior to the construction of the funnel-and-gate system, whereas the stream function values are computed for the situation after installation. The linearized uncertainty propagation relies on periodic embedding and fast Fourier transformation techniques [*Nowak et al.*, 2003; *Cirpka and Nowak*, 2004]. Depending on the spatial arrangement of the existing data and the design under investigation, we determine optimal sampling locations for additional conductivity measurements by linearized approaches. Here the optimal sample location maximizes the expected gain of information regarding the functionality of a particular system design.

2. Mathematical Methods

2.1. Governing Equations

[12] We consider two-dimensional steady state groundwater flow without internal volumetric sources or sinks, satisfying the groundwater flow equation:

$$\nabla \cdot (K \nabla h) = 0 \tag{1}$$

in which K is the hydraulic conductivity, here assumed isotropic at the local scale, and h is the hydraulic head. The boundary Γ of the domain is subdivided into a section Γ_1

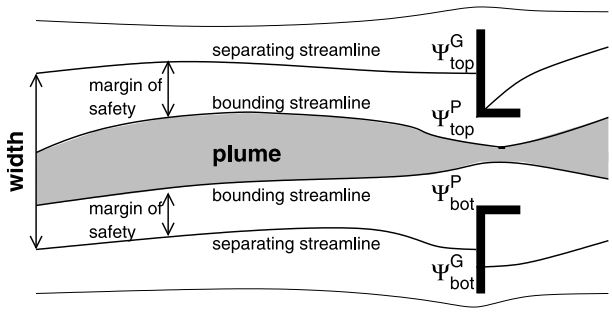

Figure 1. Stream function values as measures for the hydraulic design of a funnel-and-gate system.

with prescribed head values $\hat{h}$, and a remaining section $\Gamma\backslash\Gamma_1$ with prescribed normal flux q_Γ:

$$\begin{aligned} h &= \hat{h} \quad \text{on } \Gamma_1 \\ -\mathbf{n}\cdot(K\boldsymbol{\nabla}h) &= q_\Gamma \quad \text{on } \Gamma\backslash\Gamma_1 \end{aligned} \tag{2}$$

in which $\mathbf{n}$ is the outward pointing unit vector normal to the boundary.

[13] In two-dimensional, nondivergent flow, we can define a stream function Ψ satisfying [*Bear*, 1972, section 6.5]:

$$q_1 = \frac{\partial\Psi}{\partial x_2} \tag{3}$$

$$q_2 = -\frac{\partial\Psi}{\partial x_1} \tag{4}$$

in which q_1 and q_2 are the components of the specific-discharge vector $\mathbf{q}$ in the x_1 and x_2 directions, respectively. The stream function Ψ satisfies the following pde [*Bear*, 1972, equation (6.5.26)]:

$$\begin{aligned} \boldsymbol{\nabla}\cdot\left(\frac{1}{K}\boldsymbol{\nabla}\Psi\right) &= 0 \\ \mathbf{n}\cdot\boldsymbol{\nabla}\Psi &= 0 \quad \text{on } \Gamma_1 \\ \Psi &= \hat{\Psi} \quad \text{on } \Gamma\backslash\Gamma_1 \end{aligned} \tag{5}$$

in which the fixed value $\hat{\Psi}$ is to be determined by integration of q_Γ over the boundary $\Gamma\backslash\Gamma_1$.

[14] It is well known, that contour lines of equal stream function values are streamlines. In the given context of capturing a plume by a funnel-and-gate system, four stream function values are of interest: the two values representing the bounding streamlines of the plume, and the two values at the funnels. For illustration, see Figure 1. The discharge in a stream tube bounded by two streamlines is the difference of the two stream function values times the thickness Δz of the aquifer. Thus we can evaluate the total discharge passing through the gate from the Ψ values of the two funnels, $Q_G = \Delta z\,(\Psi^G_{top} - \Psi^G_{bot})$ in Figure 1. When a plume is captured by the gate, the difference in stream function values between the bounding streamlines and the funnels, $\Delta\Psi_{top}$ and $\Delta\Psi_{bot}$, quantify the margin of safety:

$$\Delta\Psi_{top} = \Psi^G_{top} - \Psi^P_{top} \tag{6}$$

$$\Delta\Psi_{bot} = \Psi^P_{bot} - \Psi^G_{bot} \tag{7}$$

[15] Both $\Delta\Psi_{top}$ and $\Delta\Psi_{bot}$ can take negative values. The negative values quantify how much plume-related water bypasses the funnels at the top and bottom funnels.

[16] The objective of the following analysis is to estimate the margins of safety, $\Delta\Psi_{top}$ and $\Delta\Psi_{bot}$, and their variances, $\sigma^2_{\Delta\Psi_{top}}$ and $\sigma^2_{\Delta\Psi_{bot}}$, based on uncertain information about the aquifer properties. The design is considered sufficiently reliable when $\Delta\Psi_{top} > 1.65\ \sigma_{\Delta\Psi_{top}}$ and $\Delta\Psi_{bot} > 1.65\ \sigma_{\Delta\Psi_{bot}}$ implying 95% confidence that the values are indeed positive provided that $\Delta\Psi_{top}$ and $\Delta\Psi_{bot}$ are approximately Gaussian.

2.2. First-Order Second-Moment Approximation of the Stream Function

[17] We consider the log conductivity $Y = \ln(K)$ a second-order random space variable:

$$\exp(\langle Y(\mathbf{x}_\mathrm{I})\rangle) = K_g(\mathbf{x}_\mathrm{I}) \tag{8}$$

$$\langle Y'(\mathbf{x}_\mathrm{I})Y'(\mathbf{x}_\mathrm{II})\rangle = C_{YY}(\mathbf{x}_\mathrm{I}, \mathbf{x}_\mathrm{II}) \tag{9}$$

in which $\langle\rangle$ denotes the expected value operator, primed quantities denote deviations from the expected value, K_g is the geometric mean of the conductivity which may exhibit a spatial trend, and $C_{YY}(\mathbf{x}_\mathrm{I}, \mathbf{x}_\mathrm{II})$ is the covariance function of the log conductivity fluctuations at locations $\mathbf{x}_\mathrm{I}$ and $\mathbf{x}_\mathrm{II}$. Discretizing the log conductivity field in cells of constant values, we consider the vector $\mathbf{Y}$ of discrete log conductivity values characterized by its expected value $\langle\mathbf{Y}\rangle$ and covariance matrix $\mathbf{C_{YY}}$. In general, we allow for a trend model of the expected log conductivity field:

$$\langle\mathbf{Y}\rangle = \mathbf{X}\boldsymbol{\beta} \tag{10}$$

in which $\boldsymbol{\beta}$ is a $n_b \times 1$ vector of trend parameters with the number of trend parameters n_b, and $\mathbf{X}$ is a $n_Y \times n_b$ matrix of discretized base functions with entries depending on the location $\mathbf{x}$ at which the log conductivity $Y(\mathbf{x})$ is considered. For known trend parameters $\boldsymbol{\beta}$, we assume $\mathbf{Y}$ to fluctuate about $\mathbf{X}\boldsymbol{\beta}$ with a multi-Gaussian distribution described by the covariance matrix $\mathbf{C_{YY}}$. In addition, the trend parameters $\boldsymbol{\beta}$ may be uncertain. To account for the uncertainty of $\boldsymbol{\beta}$, we assume a multi-Gaussian distribution of $\boldsymbol{\beta}$ with prior mean $\boldsymbol{\beta}^*$ and covariance $\mathbf{C}_{\beta\beta}$. Marginalization leads to the marginal mean $\mathbf{Y}^*$ and the marginal covariance matrix $\mathbf{G_{YY}}$ of $\mathbf{Y}$ with uncertain value of the drift coefficients $\boldsymbol{\beta}$:

$$\mathbf{Y}^* = \mathbf{X}\boldsymbol{\beta}^* \tag{11}$$

$$\mathbf{G_{YY}} = \mathbf{C_{YY}} + \mathbf{X}\mathbf{C}_{\beta\beta}\mathbf{X}^T \tag{12}$$

In the case that there is no information on the trend parameters whatsoever, i.e., $\mathbf{C}^{-1}_{\beta\beta} = \mathbf{0}$, the marginal variance of Y is infinite, and the marginal covariance matrix $\mathbf{G_{YY}}$ is a generalized rather than a regular covariance matrix. The inverse $\mathbf{G}^{-1}_{\mathbf{YY}}$, however, is still regular [see *Kitanidis*, 1995, and references therein]. In our application we will assume a uniform, uncertain mean of the log conductivity $Y(\mathbf{x})$. Then, $\mathbf{X}$ is a $n_y \times 1$ vector of unit entries, β is a scalar coefficient with mean β^* and variance σ^2_β, and the marginal covariance function of the log conductivity field is given by $G_{YY}(\mathbf{x}_\mathrm{I}, \mathbf{x}_\mathrm{II}) = C_{YY}(\mathbf{x}_\mathrm{I}, \mathbf{x}_\mathrm{II}) + \sigma^2_\beta$. Trend models differing from the uniform mean, such as linear trends or uniform mean

values in distinct zones, are easy to implement. The different zones may also have different covariance functions to describe the variability within [e.g., *Cirpka and Nowak*, 2004]. Applying such zonation models, however, requires that the geometry of the zones is deterministic.

[18] Since the field of stream function values $\Psi(\mathbf{x})$ depends on the random space variable $Y(\mathbf{x}_I)$, it is also a random variable which may be characterized by its expected value and covariance function. We get the zeroth-order approximation $\Psi^{(0)}(\mathbf{x})$ of the stream function $\Psi(\mathbf{x})$ in random heterogeneous media by solving for the stream function values applying the field of the expected log conductivity values:

$$\begin{aligned} \boldsymbol{\nabla}\cdot\left(\frac{1}{K_g}\boldsymbol{\nabla}\Psi^{(0)}\right) &= 0 \\ \mathbf{n}\cdot\boldsymbol{\nabla}\Psi &= 0 \quad \text{on } \Gamma_1 \\ \Psi &= \hat{\Psi} \quad \text{on } \Gamma\backslash\Gamma_1 \end{aligned} \tag{13}$$

[19] The uncertainty in $\Psi(\mathbf{x})$ can be estimated to the first order by linear error propagation [*Dettinger and Wilson*, 1981]:

$$C_{\Psi\Psi}(\mathbf{x},\mathbf{x}') = \int_\Omega\int_\Omega \frac{d\Psi(\mathbf{x})}{dY(\mathbf{x}_I)} C_{YY}(\mathbf{x}_I,\mathbf{x}_{II}) \frac{d\Psi(\mathbf{x}')}{dY(\mathbf{x}_{II})} d\mathbf{x}_{II} d\mathbf{x}_I \tag{14}$$

in which $C_{\Psi\Psi}(\mathbf{x}, \mathbf{x}')$ is the covariance function of the stream function at locations $\mathbf{x}$ and $\mathbf{x}'$, and $d\Psi(\mathbf{x})/dY(\mathbf{x}_I)$ is the sensitivity of $\Psi(\mathbf{x})$ with respect to $Y(\mathbf{x}_I)$, whereas $\int_\Omega d\mathbf{x}$ denotes integration over the entire domain. Discretizing the log conductivity field in cells of constant values, the double integrals are replaced by a quadratic matrix-matrix multiplication:

$$\mathbf{C}_{\boldsymbol{\Psi}\boldsymbol{\Psi}} = \mathbf{H}_{\boldsymbol{\Psi}}\mathbf{C}_{\mathbf{YY}}\mathbf{H}_{\boldsymbol{\Psi}}^T \tag{15}$$

in which $\mathbf{C}_{\boldsymbol{\Psi}\boldsymbol{\Psi}}$ is the covariance matrix of all considered Ψ values, $\mathbf{C}_{\mathbf{YY}}$ is the covariance matrix of the discretized log conductivity values, whereas $\mathbf{H}_{\boldsymbol{\Psi}}$ is the sensitivity matrix:

$$\mathbf{H}_{\boldsymbol{\Psi}} = \frac{d\boldsymbol{\Psi}}{d\mathbf{Y}^T} \tag{16}$$

with dimensions $n_\Psi \times n_Y$ in which n_Ψ is the number of stream function observations and n_Y the number of log conductivity values. In case of an uncertain mean value of $\mathbf{Y}$, we need to apply the marginal covariance matrix $\mathbf{G}_{\mathbf{YY}}$ instead of $\mathbf{C}_{\mathbf{YY}}$ in equation (15). In case of a conditioned Y field, as discussed below, we apply the conditional covariance matrix $\mathbf{C}_{\mathbf{YY}|\mathbf{Z}^m}$.

2.3. Evaluation of Sensitivities

[20] We evaluate the sensitivity matrix $\mathbf{H}_{\boldsymbol{\Psi}}$ by the adjoint state method [*Townley and Wilson*, 1985; *Sun*, 1994], here applied to the pde of the heads, equation (1), and the stream function, equation (5).

[21] For each location $\mathbf{x}_\ell$ of head observation, we solve for an adjoint state ψ_h satisfying:

$$\begin{aligned} \boldsymbol{\nabla}\cdot\left(K_g\boldsymbol{\nabla}\psi_h\right) &= -\delta(\mathbf{x}-\mathbf{x}_\ell) \\ \psi_h &= 0 \quad \text{on } \Gamma_1 \\ \mathbf{n}\cdot\left(K_g\boldsymbol{\nabla}\psi_h\right) &= 0 \quad \text{on } \Gamma_2 \end{aligned} \tag{17}$$

in which $\delta(\mathbf{x} - \mathbf{x}_\ell)$ is the Dirac delta function. We consider the log conductivity field to be piecewise constant within finite elements. By Y_λ we denote the log conductivity within a given element λ of volume V_λ. Then, the sensitivity of $h(\mathbf{x}_\ell)$ with respect to any Y_λ is given by:

$$\frac{\partial h(\mathbf{x}_\ell)}{\partial Y_\lambda} = -\int_{V_\lambda} K_g \boldsymbol{\nabla}\psi_h\cdot\boldsymbol{\nabla}h^{(0)} dV \tag{18}$$

That is, we solve once for the head equation, equation (1), applying the expected values of the log conductivity field. Subsequently, we solve a single adjoint equation, equation (17), for each head measurement, and evaluate the sensitivity with respect to all discretized log conductivity values Y_λ by postprocessing using equation (18). This procedure is well known as the continuous adjoint state method [see *Sun*, 1994]).

[22] We apply the same procedure to the local stream function values of interest. For each observation point $\mathbf{x}_\ell$ of the stream function Ψ, we solve for an adjoint state ψ_Ψ satisfying:

$$\begin{aligned} \boldsymbol{\nabla}\cdot\left(\frac{1}{K_g}\boldsymbol{\nabla}\psi_{\boldsymbol{\Psi}}\right) &= -\delta(\mathbf{x}-\mathbf{x}_\ell) \\ \mathbf{n}\cdot\boldsymbol{\nabla}\psi_{\Psi;} &= 0 \quad \text{on } \Gamma_1 \\ \psi_\Psi &= 0 \quad \text{on } \Gamma_2 \end{aligned} \tag{19}$$

Then, the sensitivity of $\Psi(\mathbf{x}_\ell)$ with respect to any Y_λ may be computed by:

$$\frac{\partial\Psi(\mathbf{x}_\ell)}{\partial Y_\lambda} = \int_{V_\lambda} \frac{1}{K_g}\boldsymbol{\nabla}\psi_\Psi\cdot\boldsymbol{\nabla}\Psi^{(0)} dV \tag{20}$$

2.4. Conditioning

[23] The discretized log conductivity values $\mathbf{Y}$ are correlated among each other and to the hydraulic head values. Given point measurements of the hydraulic head h or of the log conductivity Y itself, we can restrict the space of possible realizations of $\mathbf{Y}$ to those satisfying the measurements within a prescribed measurement error. To this procedure we refer as conditioning. In the following, $\mathbf{Z}$ denotes the $m \times 1$ vector of the measured quantity at the m measurement points; $\mathbf{Z}^m$ denotes the measurements themselves, which may be prone to a measurement error. $\mathbf{R}_{\mathbf{ZZ}}$ is the covariance matrix of the measurement errors. We evaluate the conditional mean, or best estimate, $\hat{\mathbf{Y}}$ and the conditional, or posterior, covariance matrix $\mathbf{C}_{\mathbf{YY}|\mathbf{Z}^m}$ given Z^m by the quasi-linear method of geostatistical inversing as outlined by *Kitanidis* [1995]. The estimate $\hat{\mathbf{Y}}$ is given in the function estimate form by:

$$\hat{\mathbf{Y}}_{k+1} = \mathbf{X}\widehat{\boldsymbol{\beta}}_{k+1} + \mathbf{C}_{\mathbf{YY}}\mathbf{H}_{\mathbf{Z},k}^T\boldsymbol{\xi}_{k+1} \tag{21}$$

in which $\widehat{\boldsymbol{\beta}}_{k+1}$ is the estimate of the trend parameters after the $(k + 1)$th iteration, $\mathbf{H}_{\mathbf{Z},k}$ is the $n_Y \times m$ sensitivity matrix of the measured quantity with respect to the Y field evaluated at the previous estimate $\hat{\mathbf{Y}}_k$, and $\boldsymbol{\xi}_{k+1}$ is a $m \times 1$

vector of weights associated with the measurements. The vectors $\hat{\beta}_{k+1}$ and ξ_{k+1} are determined by solving:

$$\begin{bmatrix} \mathbf{H}_{\mathbf{Z},k}\mathbf{C}_{\mathbf{YY}}\mathbf{H}_{\mathbf{Z},k}^T + \mathbf{R}_{\mathbf{ZZ}} & \mathbf{H}_{\mathbf{Z},k}\mathbf{X} \\ \mathbf{X}^T\mathbf{H}_{\mathbf{Z},k}^T & -\mathbf{C}_{\beta\beta}^{-1} \end{bmatrix} \begin{bmatrix} \xi_{k+1} \\ \hat{\beta}_{k+1} \end{bmatrix} = \begin{bmatrix} \mathbf{Z}^m - \mathbf{Z}(\hat{\mathbf{Y}}_k) + \mathbf{H}_{\mathbf{Z},k}\hat{\mathbf{Y}}_k \\ -\mathbf{C}_{\beta\beta}^{-1}\beta^* \end{bmatrix} \tag{22}$$

in which $\mathbf{Z}(\hat{\mathbf{Y}}_k)$ is the model prediction for the measured quantity applying the previous estimate $\hat{\mathbf{Y}}_k$. The procedure has to be repeated until convergence is reached. We stabilize the method further by adopting a special version of the Levenberg-Marquardt algorithm [*Nowak and Cirpka*, 2004]. It can be shown that the solution is the linearized Bayesian update of the prior field $\mathbf{Y}^*$ conditioned on the dependent data $\mathbf{Z}^m$ [*Kitanidis*, 1995]. Equation (22) is written here for uncertain rather than completely unknown trend parameters. For the case that there is no prior information on the drift coefficients β, the corresponding inverse covariance matrix $\mathbf{C}_{\beta\beta}^{-1}$ is a zero matrix.

[24] A lower estimate of the conditional covariance $\mathbf{C}_{\mathbf{YY}|\mathbf{Z}^m}$ is given by:

$$\mathbf{C}_{\mathbf{YY}|\mathbf{Z}^m} \geq \mathbf{C}_{\mathbf{YY}} - \begin{bmatrix} \mathbf{H}_{\mathbf{Z}}\mathbf{C}_{\mathbf{YY}} \\ \mathbf{X}^T \end{bmatrix}^T \begin{bmatrix} \mathbf{H}_{\mathbf{Z}}\mathbf{C}_{\mathbf{YY}}\mathbf{H}_{\mathbf{Z}}^T + \mathbf{R}_{\mathbf{ZZ}} & \mathbf{H}_{\mathbf{Z}}\mathbf{X} \\ \mathbf{X}^T\mathbf{H}_{\mathbf{Z}}^T & -\mathbf{C}_{\beta\beta}^{-1} \end{bmatrix}^{-1} \cdot \begin{bmatrix} \mathbf{H}_{\mathbf{Z}}\mathbf{C}_{\mathbf{YY}} \\ \mathbf{X}^T \end{bmatrix} \tag{23}$$

which is exact for linear problems. It is quite obvious that the conditional covariance matrix is nonstationary even when the unconditional covariance $\mathbf{C}_{\mathbf{YY}}$ is stationary.

2.5. Periodic Embedding and Matrix Multiplications

[25] Consider a two-dimensional domain discretized by 10^5 nodes. Then, the full covariance matrix of log conductivities would have 10^{10} entries, a sensitivity matrix $\mathbf{H}_{\mathbf{Z}}$ of ten measurements would have 10^6 elements, and the evaluation of the cross covariance $\mathbf{H}_{\mathbf{Z}}\mathbf{C}_{\mathbf{YY}}$ by standard matrix multiplications would require 10^{11} floating point operations. Even with modern computer capacities, this effort would be prohibitive. However, if the discretization of the field is regularly spaced, and the covariance function is stationary, we can apply fast Fourier transformation (FFT) techniques for the multiplication of the covariance matrix with a vector [*Dietrich and Newsam*, 1997; *Nowak et al.*, 2003]. For this purpose, the stationary field is virtually embedded into a larger, periodic field which has a (block) circulant covariance matrix [*Zimmerman*, 1989]. We only evaluate the first row $\mathbf{c}_1$ of the covariance matrix related to the embedding periodic field.

[26] Formally, we can write the multiplication of the embedded covariance matrix with a vector as:

$$\mathbf{C}_{\mathbf{YY}}\mathbf{u} = \mathbf{M}^T\mathcal{F}^{-1}(\mathcal{F}(\mathbf{c}_1) \circ \mathcal{F}(\mathbf{M}\mathbf{u})) \tag{24}$$

in which $\mathcal{F}()$ and $\mathcal{F}^{-1}()$ are the discrete Fourier transformation and its inverse, respectively, $\mathbf{a} \circ \mathbf{b}$ is the Hadamard product, i.e., the element-wise multiplication of vectors $\mathbf{a}$ and $\mathbf{b}$. Multiplication with the mapping matrix $\mathbf{M}$ and its transpose $\mathbf{M}^T$ corresponds to embedding (by zero padding) and extraction (discarding the excessive elements) of the stationary field into respectively from the periodic field. A more detailed explanation of the embedding and extraction procedures is given elsewhere [*Dietrich and Newsam*, 1997; *Nowak et al.*, 2003].

[27] The multiplication requires three fast Fourier transformations (FFT), each with a computational effort of $\mathcal{O}(n_p \log_2(n_p))$ whereas the traditional matrix-vector product requires $\mathcal{O}(n_Y^2)$ operations. Hence the periodic embedding saves computational effort and memory especially for large domains, although the embedding procedure temporarily enlarges the total domain size. In matrix-matrix multiplications, we consider each column of the right-hand matrix separately. With m columns, we need $(2\ m\ +\ 1)$ FFT operations. Extensions to certain cases of nonstationary fields are given by *Cirpka and Nowak* [2004]. These include the case of conditional covariance matrices, which is relevant in the present application.

2.6. Cross-Covariance Matrix $\mathbf{C}_{\mathbf{Y\Psi}}$ Between Log Conductivity and Stream Function Values and Covariance Matrix $\mathbf{C}_{\mathbf{\Psi\Psi}}$ of Stream Function Values

[28] We assume that the covariance function of the log conductivity fluctuations is stationary. A nonuniform mean in the log conductivity or boundary conditions in the flow problem may lead to a nonstationary velocity field. In that case, $d\Psi(\mathbf{x}_{\mathrm{I}})/dY(\mathbf{x}_{\mathrm{II}})$ depends on the actual position of $\mathbf{x}_{\mathrm{I}}$ and $\mathbf{x}_{\mathrm{II}}$ rather than on the separation vector $\mathbf{x}_{\mathrm{II}} - \mathbf{x}_{\mathrm{I}}$. This means that the sensitivity matrix $\mathbf{H}_{\mathbf{\Psi}}$ does not exhibit a simple structure, whereas the covariance matrix of the log conductivity values $\mathbf{C}_{\mathbf{YY}}$ does. The cross covariance $\mathbf{C}_{\mathbf{Y\Psi}_j}$ between all log conductivity values $\mathbf{Y}$ and a single stream function value Ψ_j is given by application of equation (24):

$$\mathbf{C}_{\mathbf{Y}\Psi_j} = \mathbf{C}_{\mathbf{YY}}\mathbf{h}_{\Psi_j}^T = \mathbf{M}^T\mathcal{F}^{-1}\left(\mathcal{F}(\mathbf{c}_1) \circ \mathcal{F}\left(\mathbf{M}\mathbf{h}_{\Psi_j}^T\right)\right) \tag{25}$$

in which $\mathbf{h}_{\Psi_j}$ is the sensitivity of Ψ_j with respect to all log conductivity values, or the jth row of the sensitivity matrix $\mathbf{H}_{\mathbf{\Psi}}$. We perform the multiplication $\mathbf{C}_{\mathbf{YY}}\mathbf{h}_{\Psi_j}^T$ for each sensitivity field $\mathbf{h}_{\Psi_j}$ in order to compute the cross covariance $\mathrm{C}_{\mathbf{Y\Psi}}$ between all log conductivity values and all stream function observations.

[29] In the conditional case, we need to evaluate the sensitivity matrix $\mathbf{H}_{\mathbf{\Psi}}$ about the conditional mean $\hat{\mathbf{Y}}$, and the conditional cross-covariance matrix $\mathbf{C}_{\mathbf{Y\Psi}|\mathbf{Z}^m}$ contains two terms [*Cirpka and Nowak*, 2004]:

$$\mathbf{C}_{\mathbf{Y\Psi}|\mathbf{Z}^m} = \mathbf{C}_{\mathbf{YY}}\mathbf{H}_{\mathbf{\Psi}}^T - \left[\mathbf{C}_{\mathbf{YY}}\mathbf{H}_{\mathbf{Z}}^T, \mathbf{X}\right] \cdot \begin{bmatrix} \mathbf{H}_{\mathbf{Z}}\mathbf{C}_{\mathbf{YY}}\mathbf{H}_{\mathbf{Z}}^T + \mathbf{R}_{\mathbf{ZZ}} & \mathbf{H}_{\mathbf{Z}}\mathbf{X} \\ \mathbf{X}^T\mathbf{H}_{\mathbf{Z}}^T & -\mathbf{C}_{\beta\beta}^{-1} \end{bmatrix}^{-1} \mathbf{L}^T \tag{26}$$

with

$$\mathbf{L} = \mathbf{H}_{\mathbf{\Psi}}\left[\mathbf{C}_{\mathbf{YY}}\mathbf{H}_{\mathbf{Z}}^T, \mathbf{X}\right] \tag{27}$$

[30] The first term in equation (26) can be computed by equation (25), whereas the second term is computationally

not very demanding if one solves first for the $n_\Psi \times (m + n_b)$ auxiliary matrix $\mathbf{L}$ according to equation (27).

[31] The covariance matrix $\mathbf{C}_{\Psi\Psi}$ of all observed stream function values is given by the matrix-matrix product:

$$\mathbf{C}_{\Psi\Psi} = \mathbf{H}_\Psi \mathbf{C}_{\mathbf{Y}\Psi} \tag{28}$$

The latter operation does not differ between the unconditional and the conditional case.

[32] In our application, the differences in stream function values $\Delta\Psi_{top}$ and $\Delta\Psi_{bot}$ according to Equations (6) and (7) describe the margins of safety. The first-order variance $\sigma^2_{\Delta\Psi_{top}}$ of $\Delta\Psi_{top}$ is:

$$\sigma^2_{\Delta\Psi_{top}} = \sigma^2_{\Psi^G_{top}} + \sigma^2_{\Psi^P_{top}} - 2C_{\Psi^G_{top}\Psi^P_{top}} \tag{29}$$

in which $\sigma^2_{\Psi^G_{top}}$ and $\sigma^2_{\Psi^P_{top}}$ are the variances of Ψ^G_{top} and Ψ^P_{top}, respectively, and $C_{\Psi^G_{top}\Psi^P_{top}}$ is the covariance. The first-order variance of $\Delta\Psi_{bot}$ is computed in an analogous way.

2.7. Cross-Covariance Between Stream Function and Head Values

[33] We now consider the covariance $C_{h\Psi}(\mathbf{x}, \mathbf{x}_j)$ between the heads $h(\mathbf{x})$ throughout the entire domain and a single stream function value $\Psi(\mathbf{x}_j)$. The procedure outlined in the following is identical for the unconditional and conditional cases. Using linear error propagation, $C_{h\Psi}(\mathbf{x}, \mathbf{x}_j)$ is given by:

$$C_{h\Psi}(\mathbf{x}, \mathbf{x}_j) = \int_\Omega \frac{\partial h(\mathbf{x})}{\partial Y(\mathbf{x}_\mathrm{I})} \underbrace{\int_\Omega C_{YY}(\mathbf{x}_\mathrm{I}, \mathbf{x}_\mathrm{II}) \frac{\partial \Psi(\mathbf{x}_j)}{\partial Y(\mathbf{x}_\mathrm{II})} d\mathbf{x}_\mathrm{II}}_{C_{Y\Psi}(\mathbf{x}_\mathrm{I}, \mathbf{x}_j)} d\mathbf{x}_\mathrm{I} \tag{30}$$

which becomes in discrete form:

$$C_{h\Psi}(\mathbf{x}, \mathbf{x}_j) = \sum_{i=1}^{n_Y} \frac{\partial h(\mathbf{x})}{\partial Y_i} C_{Y_i\Psi_j} \tag{31}$$

[34] At first, equation (31) looks computationally very demanding because of the sensitivity $\partial h(\mathbf{x})/\partial \mathbf{Y}$ of all head values with respect to all log conductivity values: Either we apply direct numerical differentiation with respect to each log conductivity value Y_i, or we apply the adjoint state method for all discretized $h(\mathbf{x})$ values. Both procedures would require solving n_Y additional groundwater flow equations. However, we are interested in a weighted sum rather than in the sensitivities of the heads with respect to the log conductivities themselves. This allows us to evaluate $C_{h\Psi}(\mathbf{x}, \mathbf{x}_j)$ for all values $h(\mathbf{x})$ by solving only a single additional groundwater equation per observation point of the stream function.

[35] Consider the direct numerical differentiation approach to compute the sensitivity of the head field $h(\mathbf{x})$ with respect to a single log conductivity value Y_i. Here we perturb the single parameter Y_i by ΔY_i, keeping all other parameters constant, and divide the difference of outcomes by the perturbation ΔY_i. We are interested in the product of $\partial h(\mathbf{x})/\partial Y_i$ and $C_{Y_i\Psi_j}$. Thus we can take a perturbation $\Delta Y_i = aC_{Y_i\Psi_j}$ that is proportional to $C_{Y_i\Psi_j}$, and divide subsequently only by the proportionality coefficient a:

$$\begin{aligned}\frac{\partial h(\mathbf{x})}{\partial Y_i} C_{Y_i\Psi_j} &\approx \frac{h(\mathbf{x}, \mathbf{Y} + \mathbf{u}_i \Delta Y_i) - h(\mathbf{x}, \mathbf{Y})}{\Delta Y_i} C_{Y_i\Psi_j} \\ &= \frac{h\left(\mathbf{x}, \mathbf{Y} + a\mathbf{u}_i C_{Y_i\Psi_j}\right) - h(\mathbf{x}, \mathbf{Y})}{a}\end{aligned} \tag{32}$$

in which $h(\mathbf{x}, \mathbf{Y})$ is the head field applying the Y field $\mathbf{Y}$ and $\mathbf{u}_i$ is the unit vector which has entries of zero everywhere except for entry i which is one. Now the weighted sum of equation (31) can be computed by:

$$C_{h\Psi}(\mathbf{x}, \mathbf{x}_j) = \frac{h\left(\mathbf{x}, \mathbf{Y} + a\mathbf{C}_{\mathbf{Y}\Psi_j}\right) - h(\mathbf{x}, \mathbf{Y})}{a} \tag{33}$$

[36] That is, we perturb the entire vector $\mathbf{Y}$ by a multiple of $\mathbf{C}_{\mathbf{Y}\Psi_j}$, compute the perturbed head field, and divide the head perturbation by the proportionality constant a between $\Delta\mathbf{Y}$ and $\mathbf{C}_{\mathbf{Y}\Psi_j}$. The coefficient a must be so small that the linear approximation is still appropriate, and so large that the heads in the perturbed case differ significantly from the unperturbed ones. In our application, we have scaled $\mathbf{C}_{\mathbf{Y}\Psi_j}$ such that the largest entry of $\Delta\mathbf{Y}$ equals 0.1.

2.8. Worth of Additional Measurement Points

[37] Consider a log conductivity field conditioned on the measurements $\mathbf{Z}^m$. The uncertainty of the estimated stream function values Ψ is expressed by the conditional covariance $\mathbf{C}_{\Psi\Psi|\mathbf{Z}^m}$. In the design of a funnel-and-gate system, we evaluate the margins of safety by the differences of stream function values between the funnel and the bounding streamline (see the application in section 3). By above mentioned techniques of uncertainty propagation, we can compute the related variance of the margin of safety. In order to reduce the uncertainty, one might take additional measurements. In the decision process, the costs of additional measurements must be justified by a sufficient decrease of the uncertainty. The exact worth of an additional measurement can, of course, only be determined after performing the measurement. Before taking the measurement, we can only assume 1) that the most likely value of the measurement will be its expected value and 2) that the linearization about the last estimate is appropriate also when we have the additional data point. On the basis of these assumptions, we can estimate the reduction in the covariance $\mathbf{C}_{\Psi\Psi|\mathbf{Z}^m}$ by linear Bayesian updating [*Rouhani*, 1985].

[38] We denote the new measurement at location $\mathbf{x}$ by $\zeta(\mathbf{x})$. In the given context, the measurement could be a log conductivity value or a hydraulic head. The (conditional) covariance of the stream function values prior to taking the measurement is denoted by $\mathbf{C}^{prior}_{\Psi\Psi}$, the cross-covariance between the stream function values and the measurement prior to taking the measurement is $\mathbf{C}^{prior}_{\Psi\zeta(\mathbf{x})}$, and the corresponding uncertainty in the measured quantity is $\sigma^2_{\zeta(\mathbf{x}),prior}$. Then, the expected conditional covariance $\mathbf{C}^{post}_{\Psi\Psi}$ of the stream function values after taking the measurement is:

$$\mathbf{C}^{post}_{\Psi\Psi} \approx \mathbf{C}^{prior}_{\Psi\Psi} - \mathbf{C}^{prior}_{\Psi\zeta(\mathbf{x})} \left(\sigma^2_{\zeta(\mathbf{x}),prior}\right)^{-1} \mathbf{C}^{prior}_{\zeta(\mathbf{x})\Psi} \tag{34}$$

which is exact only for linear problems.

[39] For log conductivity measurements, we can compute $\mathbf{C}^{post}_{\Psi\Psi}$ for all locations $\mathbf{x}$ of the measurement quite easily. Here the prior variance $\sigma^2_{Y(\mathbf{x}),prior}$ of the log conductivity is given by the diagonal entries of $\mathbf{C}_{\mathbf{YY}|\mathbf{Z}^m}$ evaluated by equation (23), and the prior cross covariance $\mathbf{C}^{prior}_{Y(\mathbf{x})\Psi}$ can be calculated for all discretized locations $\mathbf{x}$ as $\mathbf{C}_{\mathbf{Y}\Psi|\mathbf{Z}^m}$ by equation (26). That is, we can compute the reduction in

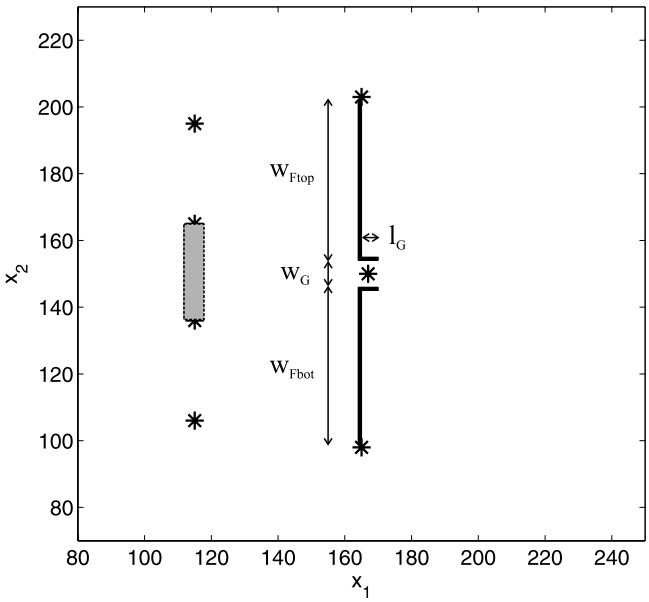

Figure 2. Base case scenario. Asterisks, locations of head and conductivity measurements; shaded rectangle, zone of contaminant source; thick lines, funnel segments of the proposed funnel-and-gate design (w_{Ftop}, width of top funnel; w_{Fbot}, width of bottom funnel; w_G, width of gate; ℓ_G, length of gate).

uncertainty, $\mathbf{C}^{prior}_{\Psi\Psi} - \mathbf{C}^{post}_{\Psi\Psi}$, for all locations $\mathbf{x}$ of the supposed log conductivity measurement, plot the result in a map and pick the location with the highest expected worth.

[40] For head measurements, mapping the worth of the measurement at all possible locations is computationally demanding. As described above, we can evaluate the cross covariance $\mathbf{C}^{prior}_{\Psi\zeta(\mathbf{x})}$, here $C_{h\Psi}(\mathbf{x}, \mathbf{x}_j)$, quite easily for all values of $\mathbf{x}$ by equation (33). However, the prior variance $\sigma^2_{h(\mathbf{x}),prior}$ requires the calculation of the sensitivity $\partial h(\mathbf{x})/\partial \mathbf{Y}$ for the specific location $\mathbf{x}$ and subsequent quadratic multiplication of the conditional covariance $\mathbf{C}_{\mathbf{YY}|\mathbf{Z}^m}$ of log conductivity values with the sensitivity $\partial h(\mathbf{x})/\partial \mathbf{Y}$. That is, for each location $\mathbf{x}$ of a possible new head measurement, we need to solve for an individual adjoint state ψ_h.

3. Application to a Hypothetical Test Case

3.1. Containment Problem and Design of Funnel-and-Gate System

[41] The methodology described above is applied to a two-dimensional synthetic model site, depicted in Figure 2. It is assumed that a contaminant plume was detected in the course of a preliminary site investigation program. This forms the base case scenario of available information. At the left transect, the plume width is estimated to 30 m. It is further hypothesized that, e.g., due to accessibility constraints, the funnel-and-gate system can only be installed 50 m downstream of the left transect. On the basis of outcrop analogues, a moderately heterogeneous, sandy aquifer is expected. It is believed that the conductivity has a geometric mean $K_g = 1.0 \times 10^{-4}$ m/s. The variance of log conductivity is assumed $\sigma^2_Y = 1.0$. The covariance of the log conductivity fluctuations follow an isotropic exponential model with correlation length $\lambda_x = \lambda_y = 15$ m. A regional hydraulic gradient $J = 0.01$ is forcing the mean groundwater flow from the left to the right. The numerical model consists of a 300 $\times$ 300 grid with quadratic elements of 1 *m* side length. The funnels are modelled as stripes of impermeable elements. For the filling of the gates, a hydraulic conductivity of 0.01 *m/s* is assumed.

[42] The dimensions and shape of the funnel-and-gate system are determined by use of a design procedure for homogeneous conditions, described by [*Teutsch et al.*, 1997]. In the preliminary design, assumptions about the type of contaminant, its concentration, and the reactive behavior of the gate are needed. Since the current study is on hydraulic failure only, we do not go into the details of the latter analysis and directly present the resulting design parameters instead. The system is placed in such a way that the middle axis of the gate and the middle axis of the detected plume fall onto the same line. The width w_G and length ℓ_G of the gate are 8 m and 5 m, respectively. The funnel is symmetric and the total funnel width $w_F = w_{Ftop} + w_{Fbot}$ (see Figure 2) is 96 m. From simulations of flow and transport under homogeneous conditions, one would approximate that the capture width of the gate is about 1.33 times the plume width.

[43] As can be seen in Figure 2, the base case scenario comprises a second investigation transect, which is placed at the proposed location of the funnel-and-gate system. The arrangement of these sampling locations is based on the design of the system. As water is forced to flow either around the funnels or through the gate, the most sensitive points of the stream function values of interest with respect to local conductivity are the end points of the funnels and the gate opening. Hence these points have been selected a priori for conductivity and head sampling.

[44] The actual measurement values of conductivity and hydraulic head were taken from selected conductivity realizations of the above mentioned geostatistical aquifer model (and calculated head fields, respectively) serving as hypothetical realities. Two realizations were selected: one is representing a "good" conductivity field (see Figure 3, bottom), so that the proposed design is capturing the plume, the other represents a "bad" conductivity field (see Figure 3, top), i.e., a situation that would lead to a design failure. On the basis of the information of the base case scenario, both realizations are equally likely. Absolute measurement errors are also accounted for but, for the sake of simplicity, are assumed to be comparatively small (standard deviation of log conductivity measurements: 0.01, of head measurements: 0.01 m).

[45] For the proposed design to be deemed successful a certain upper probability threshold of plume capture has to be reached for each plume boundary. The probability of capture is determined according to the presented methodology as follows. Two stream function values (denoted Ψ^P_{top} and Ψ^P_{bot}) are computed at the upper (top) and lower (bot) plume detection boundaries. The same is done for the upper (Ψ^G_{top}) and lower (Ψ^G_{bot}) gate boundary. Therefore plume capture is considered to be achieved, if the differences $\Delta\Psi_{top} = \Psi^G_{top} - \Psi^P_{top}$ and $\Delta\Psi_{bot} = \Psi^P_{bot} - \Psi^G_{bot}$ are positive numbers. As all the stream function values are random rather than deterministic numbers, the two

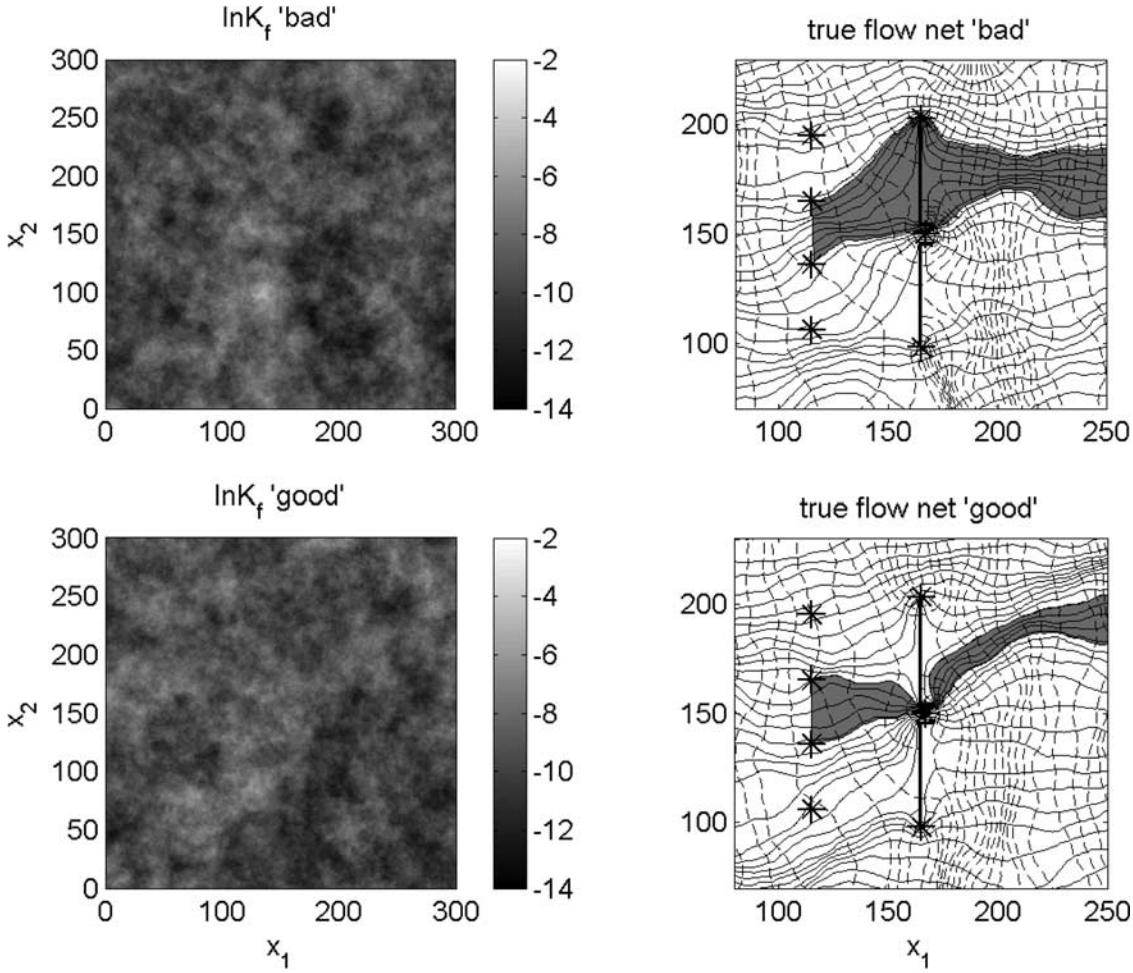

Figure 3. Bad and good virtual realities: (left) distributions of log conductivity; (right) streamline patterns (gray area marks the plume). (top) Bad case in which design fails; (bottom) Good case with successful implementation. Both aquifer realizations are conditioned to the same head and conductivity data (locations denoted by asterisks).

differences, $\Delta\Psi_{top}$ and $\Delta\Psi_{bot}$ are also random. The evaluation of the first-order variance of those differences is given by equation (29). In order to achieve a certain reliability, the probability of both $\Delta\Psi_{top}$ and $\Delta\Psi_{bot}$ has to exceed a defined critical value. Approximating the pdf of $\Delta\Psi_{top}$ as Gaussian distribution, the 95% probability of exceedance is given for $\Delta\Psi_{top} = \langle\Delta\Psi_{top}\rangle - 1.65\ \sigma_{\Psi_{top}}$, in which $\langle\Delta\Psi_{top}\rangle$ is the estimated value of $\Delta\Psi_{top}$ and $\sigma_{\Psi_{top}}$ its standard deviation. Requiring 95% confidence that $\Delta\Psi_{top}$ is positive, thus results in the following constraint:

$$\langle\Delta\Psi_{top}\rangle \geq 1.65\ \sigma_{\Psi_{top}} \tag{35}$$

or

$$CV_{\Delta\Psi_{top}} = \frac{\sigma_{\Psi_{top}}}{\langle\Delta\Psi_{top}\rangle} \lessapprox 0.6, \quad \langle\Delta\Psi_{top}\rangle > 0 \tag{36}$$

in which $CV_{\Delta\Psi_{top}}$ is the coefficient of variation. The same criterion has to be met by $\Delta\Psi_{bot}$. Of course, this limit is intended to be reached only for a successful design. In order to prove with 95% certainty that a design fails, $\langle\Delta\Psi_{top}\rangle$ or $\langle\Delta\Psi_{bot}\rangle$ must be negative, and the corresponding coefficient of variation $\gtrapprox -0.6$. This can be interpreted as abandoning the proposed design based on the knowledge of a 95% probability of failure. This is done for demonstration purposes only, as no practitioner would seek after such a high probability of failure before discarding a preliminary design.

3.2. Results of the Probability-Based Design Evaluation

3.2.1. Base Case Scenario

[46] Figure 4 shows the estimated flow net given the information of the base case, which accounts for the seven measurement points shown in Figure 2. As can be seen, it is expected that the proposed funnel-and-gate design captures the plume. The coefficient of variation for the lower gate boundary $CV_{\Delta\Psi_{bot}} = 0.3158 < 0.6$ is already within the required range. The uncertainty within the conductivity field, though, renders $CV_{\Delta\Psi_{top}} = 2.538 > 0.6$. Therefore additional sampling is needed to ensure whether the plume is captured also at the top boundary to the given probability threshold. As the top boundary criterion is decisive, we omit indexing of the coefficient of variation CV hereafter.

[47] Figure 5 shows the distribution of the expected data worth of additional log conductivity measurements for the base case scenario. Here data worth is defined as the expected decrease in the estimation variance of $\Delta\Psi_{top}$ due to a log

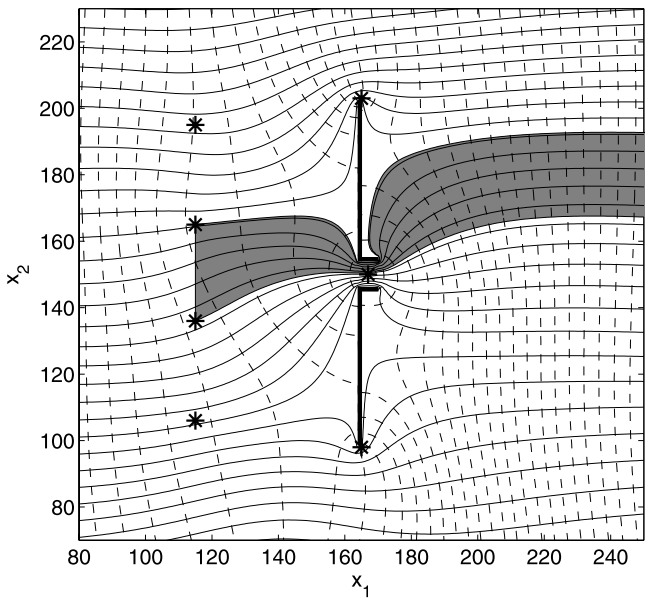

Figure 4. Estimated flow net for the proposed funnel-and-gate system design using information of the base case scenario conditioned on the seven initial measurement points. Asterisks show locations of head and conductivity measurements; gray area shows estimated plume extension.

conductivity measurement according to equation (34). Several local maxima can be distinguished. We pick the three largest local maxima as sampling locations for the next sampling phase, rather then taking one sample at a time. Head data, merely a by-product of the pumping tests performed to measure the conductivity values, are collected as well and used for the further analyses. The sampling is carried out for both true conductivity fields (i.e., the good and bad cases of the hypothetical reality), so that their outcome, and consequently the further analyses, will differ after the first sampling iteration. The evolution of the mean, standard deviation, and coefficient of variation through the different sampling campaigns are given in Table 1.

Table 1. Evolution of Estimated Mean $\langle \Delta\Psi_{top} \rangle$, Standard Deviation $\sigma_{\Delta\Psi_{top}}$, and Coefficient of Variation $CV_{\Delta\Psi_{top}}$ of $\Delta\Psi_{top}$ Through the Different Sampling Campaigns for the "Bad" and the "Good" Cases[a]

Sampling Campaign	$\langle \Delta\Psi_{top} \rangle$, $\times 10^{-6}$ m^2/s	$\sigma_{\Psi_{top}}$, $\times 10^{-6}$ m^2/s	$CV_{\Delta\Psi_{top}}$
	Bad Case		
0	3.83	9.71	2.54
1	−7.37	7.65	−1.04
2	−14.11	6.03	−0.43
	Good Case		
0	3.83	9.71	2.54
1	1.68	6.44	3.84
2	4.39	5.25	1.20
3	7.46	5.03	0.67
4	7.32	4.15	0.57

[a]True value of $\Delta\Psi_{top}$ in the bad case is 10.59×10^{-6} m^2/s; true value of $\Delta\Psi_{top}$ in the good case is $-23, 43 \times 10^{-6}$ m^2/s.

3.2.2. Assessment After the First Sampling Phase

[48] Figure 6 shows the estimated flow net after the first sampling campaign for the bad case. As can be seen, already the first three additional measurements have a strong effect on the evaluation of plume capture of the proposed design. Capture is no longer achieved for the estimated flow field, the probability of failure (defined as $Prob(\Delta\Psi_{top} \leq 0)$ with the according mean and standard deviation taken from Table 1 rises to 83% as opposed to 35% for the base case. The worth of additional data for the next sampling phase is shown in Figure 7.

[49] For the good case the first additional conditioning points lead to a slight worsening of the design performance as the probability of failure rises to 39%. Nevertheless, the standard deviation $\sigma_{\Delta\Psi_{top}}$ significantly decreased from

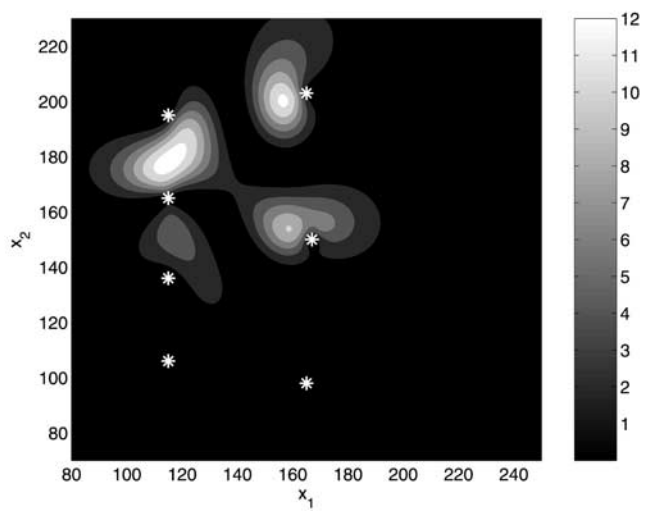

Figure 5. Data worth of additional log conductivity measurements for $\Delta\Psi_{top}$ for the base case scenario. Already existing head and conductivity data are denoted by asterisks. Multiply contour label numbers by 10^{-12} m^4/s^2.

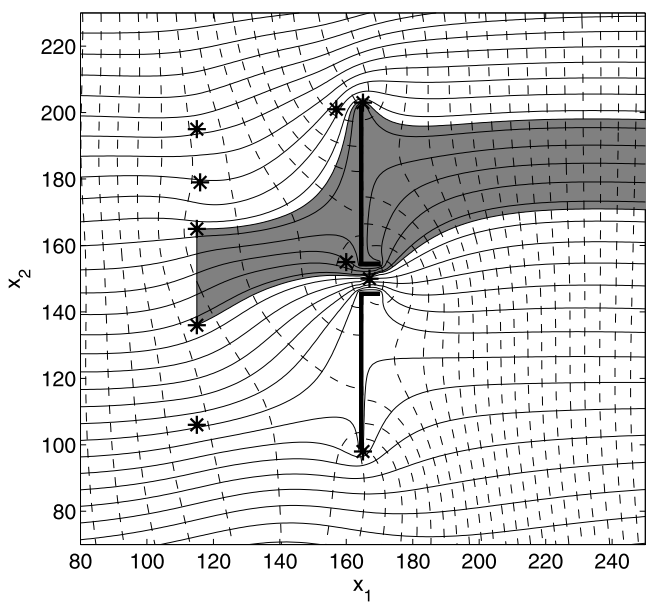

Figure 6. Estimated flow net after the first sampling campaign for the bad case. Asterisks show locations of head and conductivity measurements; gray area shows estimated plume extension.

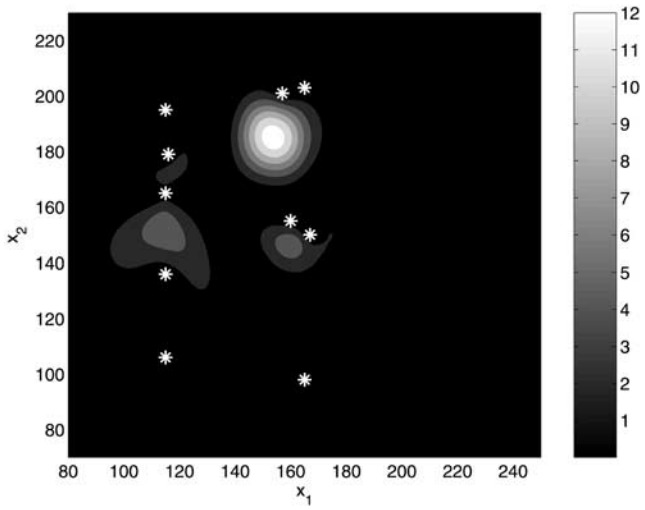

Figure 7. Data worth of additional log conductivity measurements for $\Delta\Psi_{top}$ for the bad case after the first sampling campaign. Already existing head and conductivity data are denoted by asterisks. Multiply contour label numbers by 10^{-12} m^4/s^2.

9.71×10^{-6} m^2/s to 6.44×10^{-6} (see Table 1). The worth of additional data for the good case is shown in Figure 8.

3.2.3. Further Sampling Phases

[50] For the bad case a $|CV_{\Delta\Psi_{top}}| < 0.6$ is reached with the next three samples, so that the proposed design can be rejected. The estimated flow net is shown in Figure 9. For the good case, four additional campaigns are needed compared to the bad case (see Table 1) until 95% probability for the proposed design is reached. Nevertheless, this is achieved with only 15 additional sampling points. The estimated flow net is shown in Figure 10 which may be compared to the true good flow net shown in Figure 3 (bottom right).

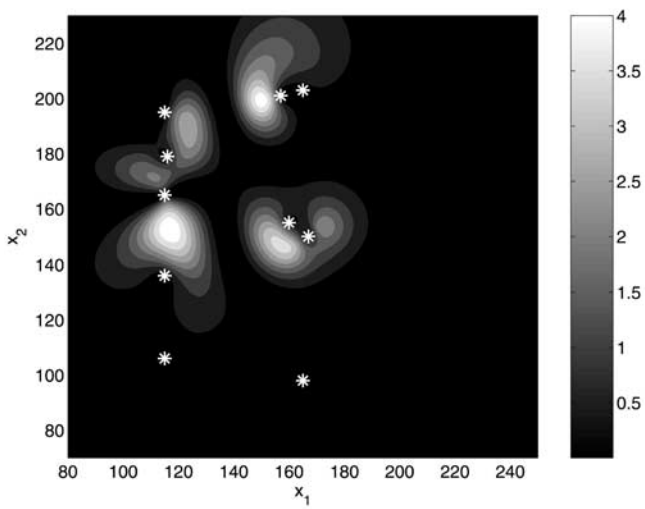

Figure 8. Data worth of additional log conductivity measurements for $\Delta\Psi_{top}$ for the good case after the first sampling campaign. Already existing head and conductivity data are denoted by asterisks. Multiply contour label numbers by 10^{-12} m^4/s^2.

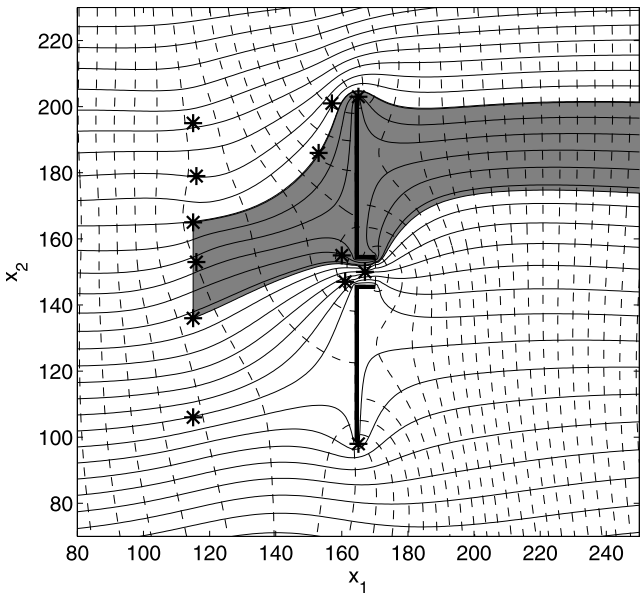

Figure 9. Estimated flow net after the second sampling campaign for the bad case. Asterisks show locations of head and conductivity measurements; gray area shows estimated plume extension.

[51] As one might expect, the gain in probability per sampling round decreases with increasing amount of conditioning points already considered. As listed in Table 1, the standard deviation of the target quantity $\Delta\Psi_{top}$ decreases in a monotonic matter, apart from a slight deviation at sampling campaign number 4. The deviation is likely to be caused by an increase in the sensitivities of the stream function values due to the new measurements, as the overall uncertainty of the conductivity is reduced. The mean $\langle\Delta\Psi_{top}\rangle$ shows an overall trend toward the true value of

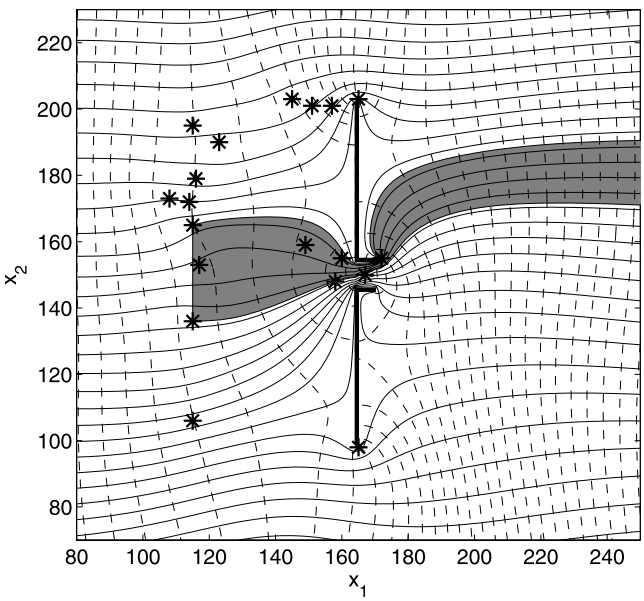

Figure 10. Estimated flow net after the fourth sampling campaign for the good case. Asterisks show locations of head and conductivity measurements; gray area shows estimated plume extension.

$\Delta\Psi_{top}$ ($\approx 1.06 \times 10^{-5}$ m^2/s), but slightly fluctuates about this trend. This may be interpreted as follows: Unlike the variance, the mean is more sensitive to the values of the measurements, and likewise a new measurement might capture a feature of the true aquifer pattern, which on its own, may dominate the model prediction, whereas within the true parameter field its effect is compensated by another, not yet captured feature. At least in the commonly encountered sparse data situation this could always be the case. Because of the slight fluctuations in the mean, the coefficient of variation $CV_{\Delta\Psi_{top}}$ counterintuitively increases with the first sampling campaign. Overall, however, the proposed sampling strategy effectively reduces the uncertainty regarding plume capture.

[52] The asterisks in Figure 9 (bad case) and Figure 10 (good case) show the sampling locations chosen based on the data worth calculations for additional conductivity measurements. It is obvious that focussing on $\Delta\Psi_{top}$ as design criterion leads to a higher sampling density in the upper part of the aquifer in both the bad and the good case. Another feature that is common to both cases is that two clusters of sampling points develop, which seem to originate from the two base case locations at the tip of the top funnel and the upper gate opening. The search progresses only gradually from these points toward the middle of the two transects (in the good case). A third cluster of sampling points seems to be oriented along the left transect increasing the field resolution there. The overall minimum spacing of the sampling points of greater than 6 m (roughly smaller than $\lambda/2$) appears to be reasonable compared to the underlying spatial correlation length of 15 m.

4. Discussion and Conclusions

[53] We have presented an efficient first-order second-moment method to evaluate the reliability of a funnel-and-gate design, honoring log conductivity and head data collected prior to the construction of the system. In contrast to previous studies [*Eykholt et al.*, 1999; *Bilbrey and Shafer*, 2001; *Elder et al.*, 2002; *Bürger et al.*, 2003], our method does not require Monte Carlo simulations. Instead, we perform linearized uncertainty propagation which, strictly speaking, is valid only for small values of the (conditional) variance of log conductivities. We are confident that first-order propagation of uncertainty is permissible in our application, because the pde of the stream function has the same structure as that of hydraulic heads, for which first-order analysis has been shown adequate up to a variance σ_Y^2 of larger than one [see *Rubin*, 2003, chapter 4].

[54] We use an advective control strategy to check the hydraulic functionality of a given funnel-and-gate design, implying that transverse dispersion can be neglected [*Mulligan and Ahlfeld*, 1999]. In contrast to other studies, however, we do not simulate advective transport itself. Since we restrict the analysis to two-dimensional steady state flow, we can analyze stream function values instead. This is quite advantageous, as the governing pde of the stream function is elliptic and directly contains the conductivity as parameter. In contrast, concentrations depend on the conductivity only indirectly, namely via the velocity field. In the context of the probability analysis, it is also advantageous that the stream function values are continuous and meaningful for both the case of successful design and that of failure. In an earlier, unpublished study, we tried to assess the reliability of the funnel-and-gate system by the total mass flux captured by the gate. The latter quantity is bounded: the maximum mass flux passing through the gate is the total mass flux of the plume, and the minimum is zero. The desired result is total capture, that is, one of the two bounds. For this condition, the standard deviation of mass flux is a very unreliable measure of uncertainty, since the pdf of mass flux is definitely non-Gaussian. By analyzing stream function values, we avoid these complications.

[55] Our method relies on efficient matrix multiplication techniques that we have presented earlier in the contexts of quasi-linear geostatistical inversing and estimation of travel time uncertainty [*Nowak et al.*, 2003; *Cirpka and Nowak*, 2004]. The present application is an extension to estimating the uncertainty of stream function values. However, by evaluating the cross covariance of stream function values for conditions with the funnel-and-gate system in operation and head values prior to the gate construction (section 2.7) and by estimating the expected worth of additional measurements (section 2.8), we go beyond our previous analyses.

[56] The results of the presented numerical study demonstrate that our data worth strategy is capable of discriminating between cases where the true plume is captured against its counterpart with only a few additional samples for a specified level of probability. Because of its computational simplicity, we have computed only the data worth of additional log conductivity measurements. We have presented how to evaluate the expected worth of a head measurement at a given location. Since the latter computation requires the solution of an additional adjoint state problem per proposed measurement point, however, it is not feasible to map the data worth of head measurements as function of the measurement location. Determining the best location of an additional head measurement requires a numerical search algorithm which we have not yet implemented.

[57] Our method is restricted to cases where two-dimensional analysis seems reasonable because, unlike its two-dimensional counterpart, a three-dimensional stream function approach is computationally and conceptually cumbersome. In most applications, the funnels vertically extend to an underlying aquitard, and the horizontal dimensions of the aquifer, and of the funnels, are much larger than the vertical. Hence the flow field essentially is horizontal. In such situations, in fact, two-dimensional analysis may be a conservative estimate with respect to horizontal plume meandering. In a two-dimensional system, the flow can pass around a low-transmissivity lens only by horizontal meandering, whereas in a three-dimensional aquifer, there is the chance of passing above or below low-conductivity lenses. This is reflected, e.g., in the corresponding values of horizontal transverse dispersion macrodispersion coefficients for heterogeneous, anistropic aquifers [*Dagan*, 1988].

[58] In future work, our data worth strategy may be combined with the optimization of the funnel-and-gate design at a given level of information. In such a step, the funnel-and-gate system would be redesigned to achieve the desired certainty that $\Delta\Psi_{top}$ and $\Delta\Psi_{bot}$ are positive numbers. Finally, the decision on taking additional samples would be based on a cost comparison between expected cost reduction

due to reduction of uncertainty versus costs of the measurements, leading to a full analysis of the expected value of sample information.

[59] **Acknowledgments.** This work was partially funded by the Emmy-Noether program of the Deutsche Forschungsgemeinschaft under the grant Ci 26/3-4. Additional funding was provided by the German Federal Ministry of Education and Research (BMBF) under the contract 02WR0195. We thank two anonymous reviewers and the associate editor handling the manuscript for their constructive remarks.

References

Andricevic, R. (1993), Coupled withdrawal and sampling designs for groundwater supply models, *Water Resour. Res.*, *29*(1), 5–16.

Bear, J. (1972), *Dynamics of Fluids in Porous Media*, Elsevier Sci., New York.

Bilbrey, L., and J. Shafer (2001), Funnel-and-gate performance in a moderately heterogeneous flow domain, *Ground Water Monit. Rem.*, *21*(3), 144–151.

Bürger, C., M. Finkel, and G. Teutsch (2003), Technical and economic evaluation of multiple gate funnel-and-gate systems under homogeneous and heterogeneous aquifer conditions, in *Calibration and Reliability in Groundwater Modelling: A Few Steps Closer to Reality (Proceedings of ModelCARE 2002, Czech Republic, 17–20 June 2002)*, *IAHS Publ.*, *277*, 448–455.

Christakos, G., and B. Killam (1993), Sampling design for classifying contaminant level using annealing search algorithms, *Water Resour. Res.*, *29*(12), 4063–4076.

Cirpka, O., and W. Nowak (2004), First-order variance of travel time in non-stationary formations, *Water Resour. Res.*, *40*, W03507, doi:10.1029/2003WR002851.

Dagan, G. (1988), Time-dependent macrodispersion for solute transport in anisotropic heterogeneous aquifers, *Water Resour. Res.*, *24*(9), 1491–1500.

Day, S., S. O'Hannesin, and L. Marsden (1999), Geotechnical techniques for the construction of reactive barriers, *J. Hazard. Mater.*, *67*, 285–297.

Dettinger, M., and J. Wilson (1981), First order analysis of uncertainty in numerical models of groundwater flow: 1. Mathematical derivation, *Water Resour. Res.*, *17*(1), 149–161.

Dietrich, C., and G. Newsam (1997), Fast and exact simulation of stationary Gaussian processes through circulant embedding of the covariance matrix, *SIAM J. Sci. Comput.*, *18*(4), 1088–1107.

Elder, C., C. Benson, and G. Eykholt (2002), Effects of heterogeneity on influent and effluent concentrations from horizontal permeable reactive barriers, *Water Resour. Res.*, *38*(8), 1152, doi:10.1029/2001WR001259.

Eykholt, G. R., C. Elder, and C. Benson (1999), Effects of aquifer heterogeneity and reaction mechanism uncertainty on a reactive barrier, *J. Hazard. Mater.*, *68*, 73–96.

Freeze, R., B. James, J. Massmann, T. Sperling, and L. Smith (1992), Hydrogeological decision analysis: 4. The concept of data worth and its use in the development of site investigation strategies, *Ground Water*, *30(4), 574–588.*

Gavaskar, A. (1999), Design and construction techniques for permeable reactive barriers, *J. Hazard. Mater.*, *68*, 41–71.

James, B., and S. Gorelick (1994), When enough is enough: The worth of monitoring data in aquifer remediation design, *Water Resour. Res.*, *30*(12), 3499–3513.

Kitanidis, P. K. (1995), Quasi-linear geostatistical theory for inversing, *Water Resour. Res.*, *31*(10), 2411–2419.

Loaiciga, H., R. Charbeneau, L. Everett, G. Fogg, B. Hobbs, and S. Rouhani (1992), Review of ground-water quality monitoring network design, *J. Hydraul. Eng.*, *118*(1), 11–37.

McGrath, W., and G. Pinder (2003), Search strategy for groundwater contaminant plume delineation, *Water Resour. Res.*, *39*(10), 1298, doi:10.1029/2002WR001636.

McMahon, P., K. Dennehy, and M. Sandstrom (1999), Hydraulic and geochemical performance of a permeable reactve barrier containing zero-valent iron, Denver Federal Center, *Ground Water*, *37*(3), 396–404.

Meyer, P., and E. Brill (1988), A method for locating wells in a groundwater monitoring network under conditions of uncertainty, *Water Resour. Res.*, *24*(8), 1277–1282.

Mulligan, A., and D. Ahlfeld (1999), Advective control of groundwater contaminant plumes: Model development and comparison to hydraulic control, *Water Resour. Res.*, *35*(8), 2285–2294.

Nowak, W., and O. Cirpka (2004), A modified Levenberg-Marquardt algorithm for quasi-linear geostatistical inversing, *Adv. Water Resour.*, *27*(7), 737–750.

Nowak, W., S. Tenkleve, and O. Cirpka (2003), Efficient computation of linearized cross-covariance and auto-covariance matrices of interdependent quantities, *Math. Geol.*, *35*(1), 53–66.

Richards, P. (2002), Construction of a permeable reactive barrier in a residential neighborhood, *Remediation*, *12*(4), 65–79, doi:10.1002/rem.10046.

Rouhani, S. (1985), Variance reduction analysis, *Water Resour. Res.*, *21*(6), 837–846.

Rubin, Y. (2003), *Applied Stochastic Hydrogeology*, Oxford Univ. Press, New York.

Sedivy, R., J. Shaker, and L. Bilbrey (1999), Design screening tools for passive funnel and gate systems, *Ground Water Monit. Rem.*, *19*(1), 125–133.

Starr, R., and J. Cherry (1994), In situ remediation of contaminated ground water: The funnel-and-gate system, *Ground Water*, *32*(3), 465–476.

Sun, N.-Z. (1994), *Inverse Problems in Groundwater Modeling*, *Theory Appl. Transp. Porous Media Ser.*, vol. 6, Kluwer Acad., Norwell, Mass.

Teutsch, G., J. Tolksdorff, and H. Schad (1997), The design of in situ reactive wall systems—A combined hydraulic-geochemical-economical simulation study, *Land Contam. Reclam.*, *5*(2), 125–130.

Townley, L. R., and J. L. Wilson (1985), Computationally efficient algorithms for parameter estimation and uncertainty propagation in numerical models of groundwater flow, *Water Resour. Res.*, *21*(12), 1851–1860.

Zimmerman, D. (1989), Computationally exploitable structure of covariance matrices and generalized covariance matrices in spatial models, *J. Stat. Comput. Simul.*, *32*(1/2), 1–15.

C. M. Bürger and M. Finkel, Center for Applied Geoscience, Universität Tübingen, Sigwartstrasse 10, D-72076 Tübingen, Germany. (claudius.buerger@uni-tuebingen.de; michael.finkel@uni-tuebingen.de)

O. A. Cirpka, Swiss Federal Institute for Environmental Science and Technology (EAWAG), Überlandstrasse 133, CH-8600 Dübendorf, Switzerland. (olaf.cirpka@eawag.ch)

W. Nowak, Institut für Wasserbau, Universität Stuttgart, Pfaffenwaldring 61, D-70550 Stuttgart, Germany. (wolfgang.nowak@iws.uni-stuttgart.de)